Title
INFLUENCE OF THE CONTINUOUS AND DISPERSED PHASES ON THE SYMMETRY OF A GAS-TURBINE AIR-BLAST ATOMIZER

Journal
JOURNAL OF ENGINEERING FOR GAS TURBINES AND POWER-TRANSACTIONS OF THE ASME, 112(1)

ISSN
0742-4795

ISBN
9780791879153

Authors
MCDONELL, VG
SAMUELSEN, GS

Publication Date
1990

DOI
10.1115/1.2906476

THE AMERICAN SOCIETY OF MECHANICAL ENGINEERS
345 E. 47 St., New York, N.Y. 10017

89-GT-303

Influence of the Continuous and Dispersed Phases on the Symmetry of a Gas Turbine Air-Blast Atomizer

V. G. McDONELL and G. S. SAMUELSEN
Department of Mechanical Engineering
University of California, Irvine
Irvine, California 92717

ABSTRACT

Current trends in liquid-fueled practical combustion systems are leaving less tolerance for fuel injection deficiencies such as poor spray field symmetry. The present paper evaluates the symmetry of the flowfield produced by a practical air-blast atomizer. Specifically, the influence of both the continuous phase and dispersed phase on the sprayfield symmetry is assessed. In the present case, asymmetry in volume flux is associated principally with disparities in the injection of the dispersed phase, which is manifested by a maldistribution of larger drops. Asymmetries observed in the continuous phase without the dispersed phase are reduced in magnitude by the presence of the dispersed phase, but still contribute to asymmetry in radial spread of the dispersed phase.

INTRODUCTION

The need to assess spray field symmetry in liquid-fueled combustion systems is gaining importance for several reasons. First, the move to fuel flexible systems and smaller geometries leaves less tolerance for local variation in combustor performance due to atomizer asymmetry. Second, the current development of numerical codes for liquid-fueled systems is predicated on the assumption of spray field symmetry. Third, the measurement of droplet size and velocity typically assumes spray symmetry with the concomitant acquisition of data along a single radius rather than a full diameter. The interpretation of such data is jeopardized in the absence of atomizer symmetry.

The spray fields produced by air-assist or air-blast atomizers are a result of considerable two-phase interaction. Therefore, it is important to assess the role of each phase in order to understand the generation of any asymmetry present. Recently introduced modern diagnostics, coupled with conventional methods, portend the capability of providing the needed assessment of symmetry of the dispersed phase in both isothermal and combustor environments. Recent results have demonstrated the potential of these modern diagnostics in both environments (e.g., McDonell, et al., 1987).

The objective of the research reported in the present paper is to explore the extent to which the dispersed and continuous phases contribute to the symmetry of an air-blast atomizer using modern methods in an isothermal environment. This study provides a baseline against which the performance of the same atomizer under reacting conditions may be compared.

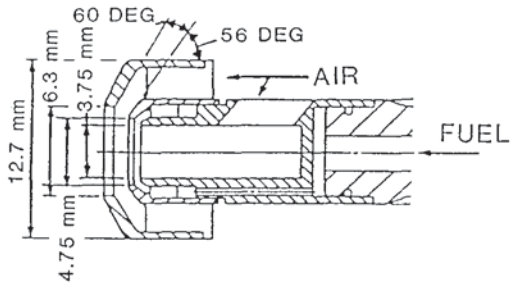

Fig. 1. Fuel Injector.

EXPERIMENT

Atomizer

The atomizer selected for characterization, shown in Figure 1, is a production air-blast atomizer for use in a production helicopter gas-turbine engine (Mongia and Reider, 1985). The atomizer features non-swirled, centrally injected air and, via an outer shroud, swirling external air. The fuel is filmed onto a circular surface (via six ports which inject the fuel tangentially in the same direction as the swirled air) and sheared between the two air passages.

Methanol is the liquid fuel used in the present study. It is selected due to suitability of the resultant data for modelling. In particular, the methanol vapor is nearly the same density as air (1.33 vs 1.2 kg/m^3) and, when injected at -10 ^{o}C (-10 ^{o}C is the wet bulb temperature at test conditions), evaporates isothermally and thereby eliminates density gradients in the gaseous environment and temperature gradients within the droplets. The atomizer is operated at an air-to-fuel ratio of 1.0 and a mass flow of 0.0021 kg/sec for each phase. The pressure drops across the atomizer are 5600 Pa and 125 Pa for the fuel and air respectively.

Spray Characterization Facility

A schematic of the test facility is shown in Figure 2. The diagnostics remain fixed, oriented about a square cutout in the optical table which measures 900 x 900 mm. The test article is directed downward from the end of a 28 mm tube which supplies

Presented at the Gas Turbine and Aeroengine Congress and Exposition—June 4-8, 1989—Toronto, Ontario, Canada
This paper has been accepted for publication in the Transactions of the ASME
Discussion of it will be accepted at ASME Headquarters until September 30, 1989

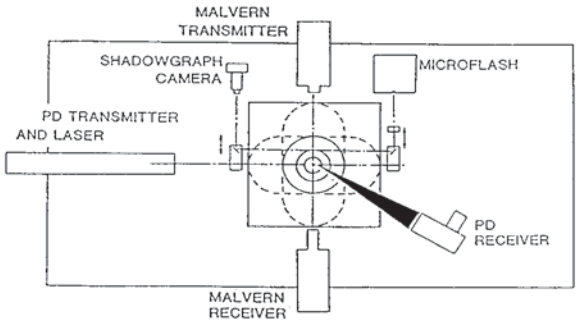

Fig. 2. Facility.

fuel and atomizing air to the atomizer. This tube is connected to a vertical traverse to provide translation in the axial direction. The entire axial traversing system is attached to the bottom of the table via a two-dimensional horizontal traverse system. Hence, three degrees of translational freedom are available to the test article. In addition, the fuel tube can be rotated about the axial centerline to any degree of atomizer orientation.

A plexiglas and flexible plastic enclosure surrounds the entire traversing/support system and ensures a stagnant environment by isolating the flowfields studied from room perturbations. This structure also permits seeding of the air entrained by the flowfields, thereby enabling unbiased measurements of the gas phase to be made. Air is introduced into the structure is removed via an exhaust system located in the fuel collection plenum. A stainless mesh separates the exhaust entrance from the structure to ensure that the exhaust suction in distributed over the large area of the plenum.

Diagnostics

Measurements of mean and fluctuating velocities for each phase are made using a two-component phase/Doppler system (Aerometrics Model 2100-3). The principal of operation of the instrument has been described in detail elsewhere (Bachalo and Houser, 1984). A schematic of the transmitter and receiver is shown in Figure 3. The measurement of the size of spheres is based upon a linear relationship between the spatial phase shift of the scattered fringe pattern and the diameter of the scatterer. The velocity is determined from the frequency of the swept fringe pattern. Comparative studies with diffraction (e.g., McDonell et al., 1987, Dodge et al., 1987), visibility (Jackson and Samuelsen, 1987), and extinction (Young and Bachalo, 1987) techniques have demonstrated good size measurement capability. In most cases, the phase Doppler approach demonstrated advantages over the other techniques.

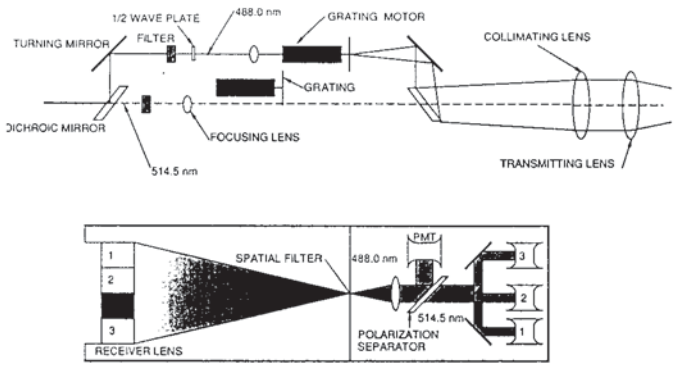

Fig. 3. Two-Component Phase Doppler Transmitter and Receiver.

Discrimination of the continuous and dispersed phases is achieved by sizing all particles including the seed particles used to track the continuous phase. Al_2O_3 (nominally 1.0 μm) is used to seed the air streams). The seed particles produce size measurements which are less than 3 μm. Using these scores and those from droplets which are less than 3 μm in diameter, statistics for the continuous phase are generated. This approach has been applied successfully in previous studies of both monodispersed (e.g., Bulzan, 1988; Mostafa et al., 1988) and polydispersed (e.g., McDonell and Samuelsen, 1988; Rudoff and Bachalo, 1988) flows. In the regions of the flowfield studied in the present work (50mm and further downstream), particles less than 3 μm in diameter track the flow to a good degree.

In addition, the instrument utilizes information from the signals obtained to generate an in-situ measurement of the probe volume cross section. Recent studies have shown that (1) developments in the methods to deduce the sampling cross section have resulted in accurate volume flux calculations in high number density flows (Bachalo et al., 1988), and (2) the values of mass flux correspond in magnitude and trend with those obtained through typical intrusive sampling techniques such as patternation (e.g., McDonell et al., 1987). In the present study, the optical technique alone is used for the volume flux measurement in lieu of a physical probe since the equivalent information is obtained with regard to fuel distributions and, in addition, details are provided with respect to size and velocity distributions. It would not be practical to conduct a detailed mapping such as the one done in the present study if volume flux were the sole quantity sought. In this case, a well developed patternation system (e.g., McVey et al., 1987), would be more appropriate.

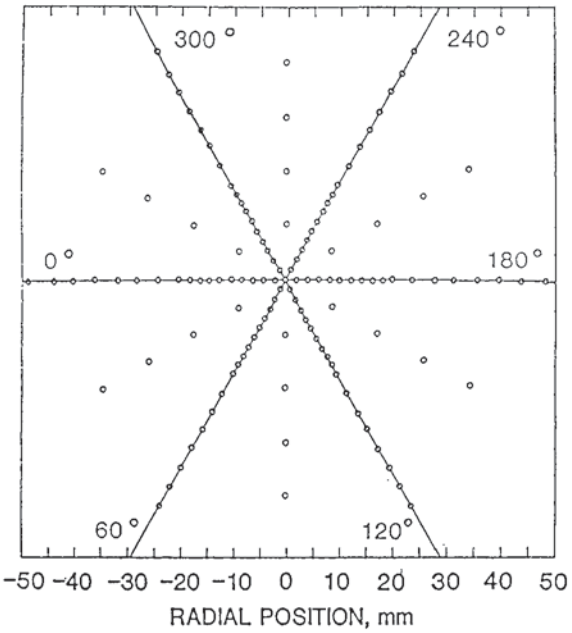

Fig. 4. Measurement Locations for Each Axial Station.

APPROACH

The approach taken in the current study is to precisely characterize the flowfield produced by a production air-blast atomizer. The first step is to conduct a three dimensional characterization of the single phase flow produced by the injector when running the nominal atomization air flow in the absence of fuel. Next, the flowfield with the injected liquid is characterized in the same three dimensional manner. The two phase characterization includes the mapping and measurements of statistics for both the liquid and dilute phase. The trends

associated with the single and two phase flows are then examined in detail to (1) provide understanding of the two-phase interaction and (2) give insight as to the cause and perpetration of asymmetries present in the flow. The characterization consists of measurements of axial and azimuthal velocity for each phase present, and particle size distribution of the dispersed phase, when present. The measurements are conducted at three axial stations(50, 75, and 100mm), and at 6 angular orientations of the atomizer (0, 60, 120, 180, 240, and 300°) at each axial station. In addition, measurements of partial profiles are conducted at 30 degree increments to ensure adequate coverage of the flowfield. Data are acquired at between 10 and 20 radial stations at each axial station depending on the radial extent of the spray field. Figure 4 shows the locations at which measurements were conducted at each axial station, and provides a reference for the location of each angular orientation.

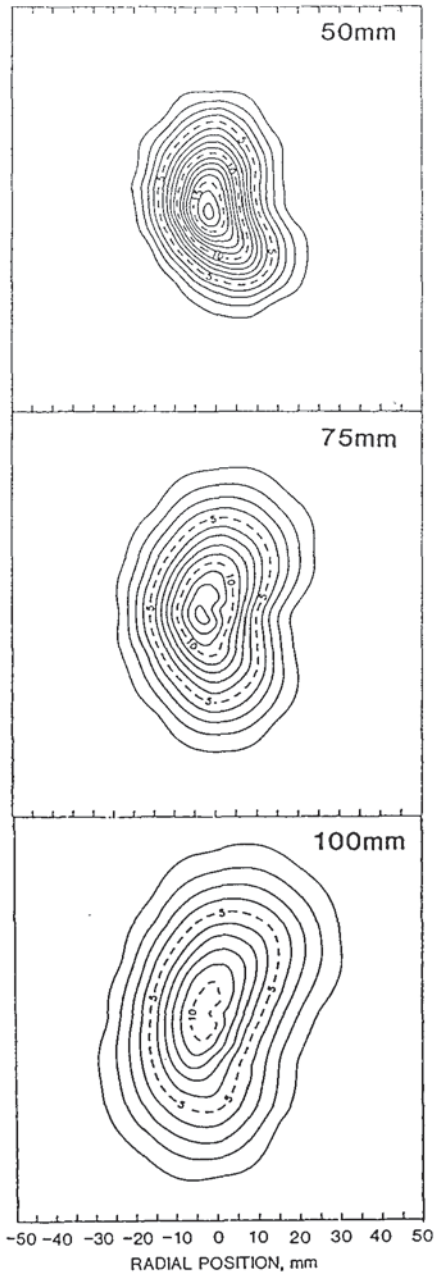

Fig. 5. Isopleths of Single Phase Axial Velocity (m/s).

RESULTS

Results are presented first for the single phase flow, followed by the continuous phase in the two-phase flow, and finally for the dispersed phase in the two-phase flow. Results are presented in either three dimensions or two dimensions. In the cases where two dimensions are presented, the results are obtained by averaging the data acquired for the six orientations unless explicitly stated as being a profile obtained from a particular orientation.

Symmetry of the Single Phase Flow

The flowfield symmetry of the atomizer was first characterized in the absence of liquid phase injection to provide a baseline against which to compare the two-phase flow results. Figure 5 shows isopleths of the mean axial velocity at three axial stations: 50, 75, and 100mm. The plots have an elliptical shape at each location. For the 50mm case, the major axis of the elliptical shape runs from 300 to 120 degrees. The ellipsoidal shape moves through approximately 40 degrees of rotation with increasing axial distance. The rotation is due to the azimuthal component of velocity imparted by the swirl vanes in the atomizer.

Figure 6 presents profiles of the mean azimuthal velocity for the six angular orientations of the atomizer studied. Figure 6a presents the data for the 50mm axial station. The extension of the ellipsoid is correlated to the presence of an asymmetry in the azimuthal velocity. Note that the azimuthal velocities associated with the 120 and 300 angular orientations are significantly higher. The 0-degree orientation has the least amount of radial spread and it also possesses the lowest azimuthal velocities. By 100mm, as shown in Figure 6b, the local peaks in azimuthal velocity has rotated clockwise to the 240 and 60 degree orientations. Again, the radial spread at these orientations is greater than that at the other orientations. At 100mm the asymmetry in azimuthal velocity is still noticeable, but is substantially damped out.

a) 50 mm Axial Station

b) 100 mm Axial Station

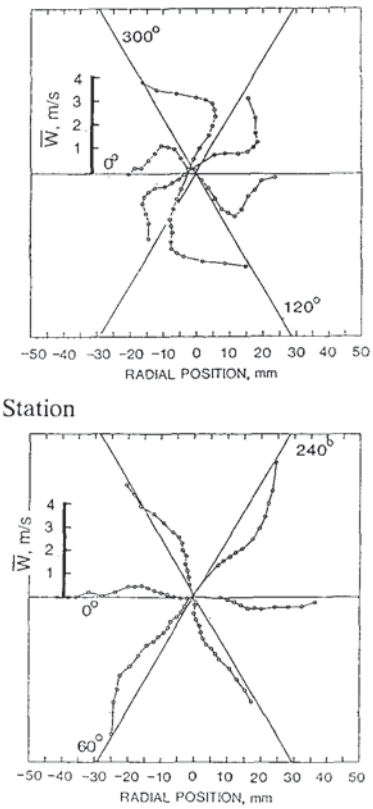

Fig. 6. Single Phase Mean Azimuthal Velocity Profiles.

Symmetry of the Two-Phase Flow

Continuous Phase. Figure 7 presents isopleths of the mean axial velocity for the continuous phase in the methanol spray field. Note that the presence of the liquid ("dispersed") phase has virtually eliminated the asymmetry present in the single phase axial velocity field. The flowfield at 50mm is nearly circular, and the elliptical behavior exhibited by the single phase flow in the absence of liquid injection is not discernable. Note that the axial velocities associated with the two-phase flow are greater at the centerline region and less at the outer edge, indicating that the presence of the spray increases the gradients in the continuous phase axial velocity.

Figure 8 presents radial profiles (averages of each of the seven orientations) of the axial turbulence intensity based upon the centerline value of the mean velocity at each axial station. The presence of the dispersed phase decreases the turbulence intensity of the continuous phase by 30%, resulting in decreased velocity decay and spread in the flow.

Figure 9 presents the azimuthal velocity profiles associated with the axial velocity isopleths of Figure 7. The 50mm axial station possesses reasonable symmetry in the azimuthal velocities, a result consistent with the symmetric axial velocity field. However, the azimuthal velocities at 120 and 300 degrees are slightly higher, a result which is consistent with the single phase flow.

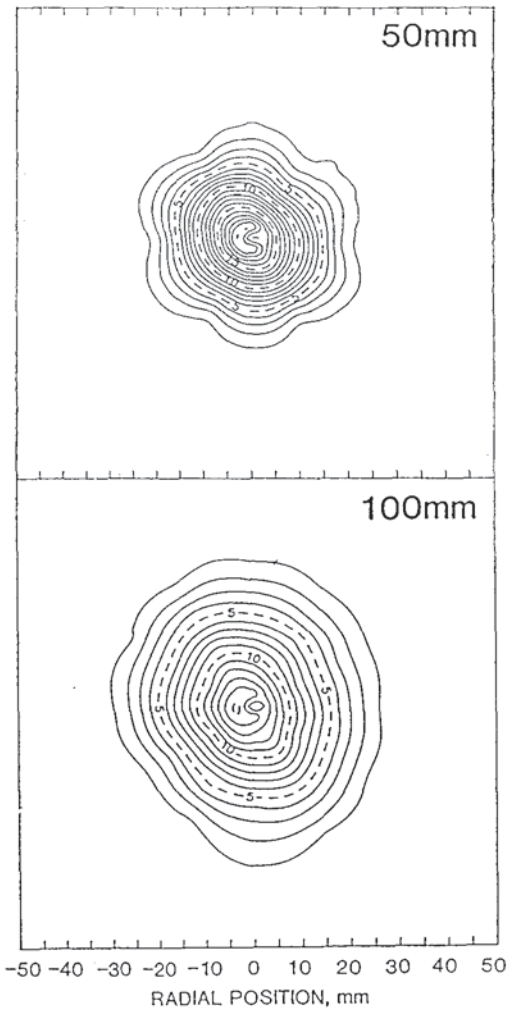

Fig. 7. Isopleths of Continuous Phase Axial Velocity (m/s).

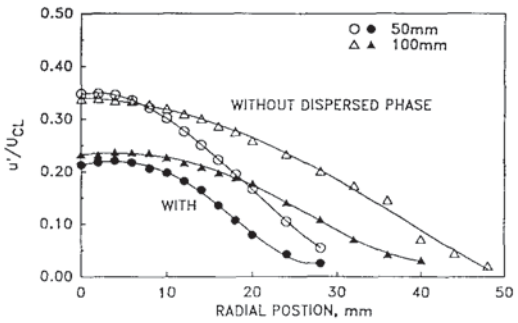

Fig. 8. Continuous Phase Turbulence Intensity.

The azimuthal velocities at 100mm are presented in Figure 9b. Note that the azimuthal velocities for the two-phase flow are slightly greater than the single phase flow at 100mm (Figure 6). The swirl is maintained a greater axial distance in the presence of the dispersed phase due to (1) the decrease of turbulence and (2) the momentum transfer between phases (the methanol is injected with swirl, concurrent with the air). At 100mm, the peak azimuthal velocities occur at 240 degrees and the minimum at 0 and 180 degree orientations, again reflecting results obtained for the single phase flow. It is noteworthy that the relatively strong azimuthal velocities at 60 degrees for the single phase flow are not present in the two-phase flow, suggesting that the disparity in the two-phase case is affected by the presence of the dispersed phase. These results demonstrate that, in the present case where equal mass is present each phase, the continuous phase is strongly influenced by the presence of the dispersed phase. One trait that persists from the single to the two-phase flow is the location of peak azimuthal velocities.

a) 50 mm Axial Station

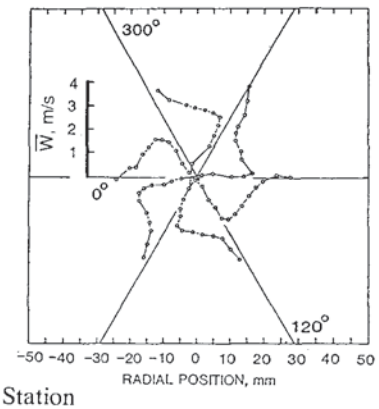

b) 100 mm Axial Station

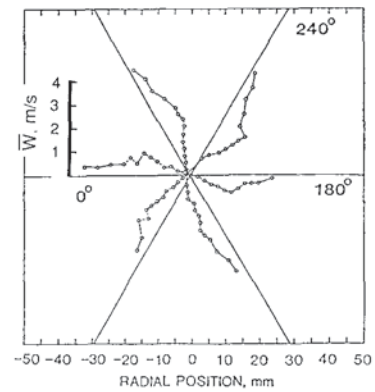

Fig. 9. Continuous Phase Mean Azimuthal Velocity Profiles.

Dispersed Phase. Isopleths of the volume flux at the 50 and 100mm stations are presented in Figure 10. The hatchure marks on the figure indicate the direction of negative gradients. Thus, the contours nearest the centerline are of lower value than those further from the centerline. The hatchure marks in this case indicate that the nozzle is hollow-cone in nature. The results at 50mm (Figure 10a) show that the uniformity in radial spread of the dispersed phase. Note also that the volume flux peaks at the 240 degree orientation. The same results are presented in Figure 10b at the 100mm axial station. By 100mm, the uniformity in radial spread has degraded. The regions from 120 through 270 degrees have considerably more radial spread than do the other regions. The location of the increased radial spread corresponds to the highest value azimuthal velocity profile (240 degrees) in both the single and two phase flows. In addition, the local peak in volume flux has rotated slightly and elongated, showing the rotation and spreading induced by the swirl.

To check the accuracy of the flux measurement, the volume under the contour surface is calculated to provide the total flow rate at each axial station. At 50mm, the integrated flow is 30% of the measured flow to the atomizer. At 100mm, it is 93% of the measured flow to the atomizer. The value at 100mm indicates good conservation of mass, especially if evaporation effects are considered. The value at 50mm, however, does not indicate mass conservation. The possible reasons for this in the present flow are numerous, and include 1) the three dimensionality of the flow which may lead to erroneous sample area determinations, and 2) relatively high concentration of droplets at the 50mm station which leads to erroneous rejection of samples. A smaller sampling volume at 50mm would likely reduce the error due to the latter reason.

a) 50 mm Axial Station

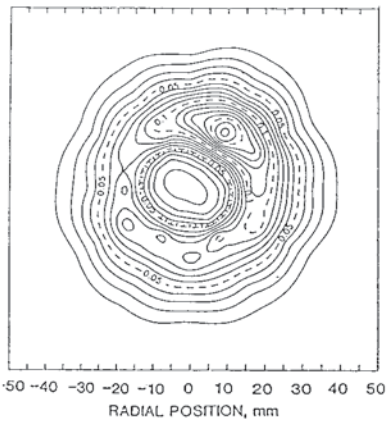

b) 100 mm Axial Station

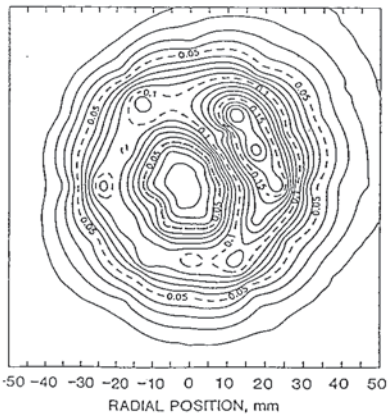

Fig. 10. Isopleths of Volume Flux (cc/cm^2sec).

Examination of the 240^o and 0^o Profiles

To better understand the relationship between the phases and the local peak in volume flux, individual profiles are now examined. Results are presented for the 240 and 0 degree orientations, since the greatest disparity in volume flux and radial spread occurs between these orientations. In particular, drop distribution means and drop distributions are examined to better understand the volume flux differences. Additional insight regarding radial spread is also provided by examination of the air/droplet velocity relationships

Volume Flux. Figures 11a and 11b present the individual radial profiles obtained for the volume flux at the orientation of greatest disparity. At 50mm and 100mm, the maximum flux occurs for either orientation from between 10 and 30mm radially. The peak flux occurs at 20 and 24mm for 50 and 100mm respectively. To examine the data with respect to percentage differences, plots of the volume flux at 240 degrees divided by the volume flux at 0 degrees are presented in Figure 12. From this figure, the disparity between orientations is clearer. From 2 to 3 times more flux are present at the regions of maximum flux (radial positions between 10 and 30mm) for 50mm and from 1 to 2 times more at 100mm. At 100mm, the disparity increases beyond 30mm radially, with up to 4 times more flux occurring for the 240 degree orientation.

At least two factors affect the volume flux directly: drop size and number of drops. Each of these factors is now examined in order to deduce the importance of each on generating the disparity between these two orientations.

a) 50 mm Axial Station

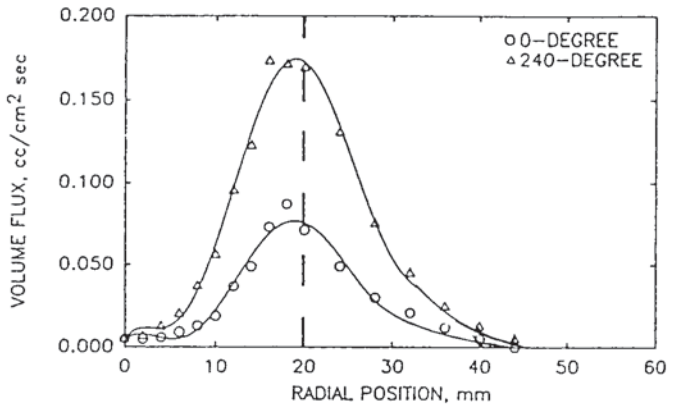

b) 100 mm Axial Station

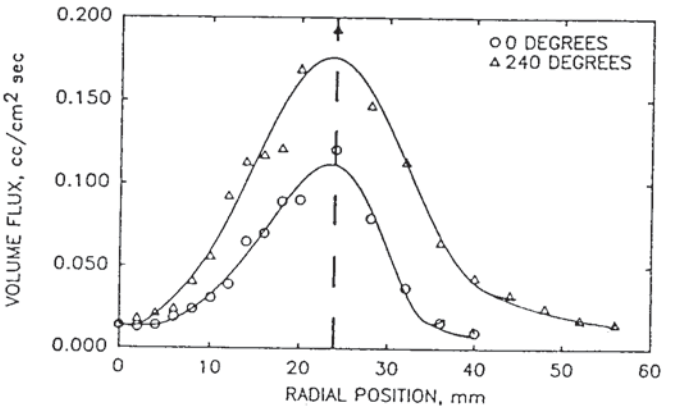

Fig. 11. Radial Profiles of Volume Flux.

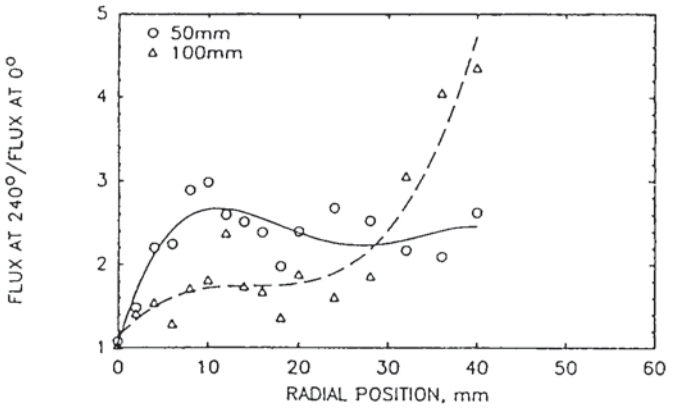

Fig. 12. Ratio of Volume Flux at 240 Degrees to Volume Flux at 0 Degrees.

i. Drop Size. In the consideration of disparities in volume flux, the best description of the drop size in the distribution at each point of the volume mean diameter or D_{30}. Radial profiles at 50 and 100mm of the ratio of the volume mean at the 240 degree orientation to the 0 degree orientation are presented in Figure 13. At both 50mm or 100mm, the discrepancy in the volume mean does not exceed 40% at any given radial position. At 50mm, the distribution volume mean at 240 degrees is between 20 and 40% higher than that at 0 degrees at radial locations corresponding to the greatest volume flux (between 12 and 28mm). This corresponds to 73 to 173% more volume flux at the 240-degree orientation. These differences nearly account for 150% greater volume flux at 240 degree orientation. At 100mm, the volume mean at the radial locations of greatest flux is 20 to 25% higher for the 240 degree orientation, corresponding to 70-95% more volume flux. These differences account for the 60 to 80% more volume flux on the 240-degree orientation between 12 and 28mm radially. However, at radial locations beyond 28mm, the difference in volume mean is not enough to account for the difference in volume flux.

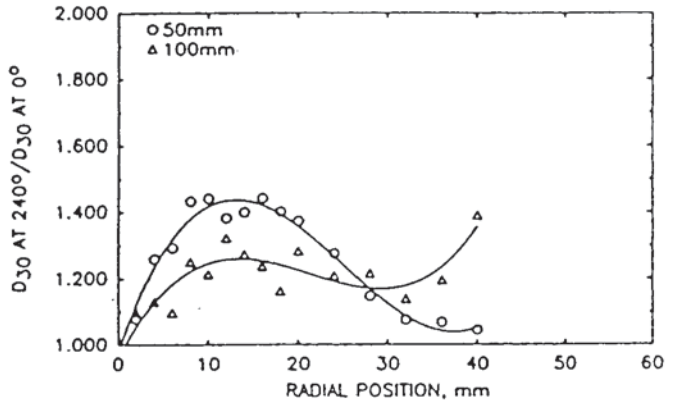

Fig. 13. Ratio of D_{30} at 240 Degrees to D_{30} at 0 Degrees.

ii. Drop Population. To identify the extent to which various droplet size groups are responsible for the disparity in volume flux, droplet size distributions and droplet volume distributions are presented in Figures 14 and 15 respectively. The distributions presented are normalized to account for variation in collection time, probe volume area, and system sensitivity as a function of drop size. As a result, the distributions presented reflect identical sensitivity and collection time, and can be used to assess the relative number of drops and volume of drops from point to point.

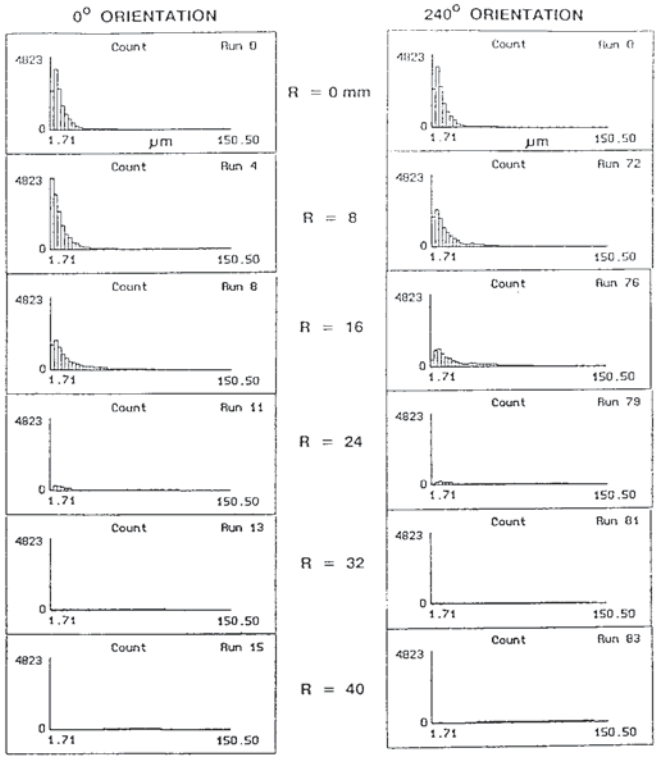

Fig. 14. Normalized Droplet Size Distributions (100mm).

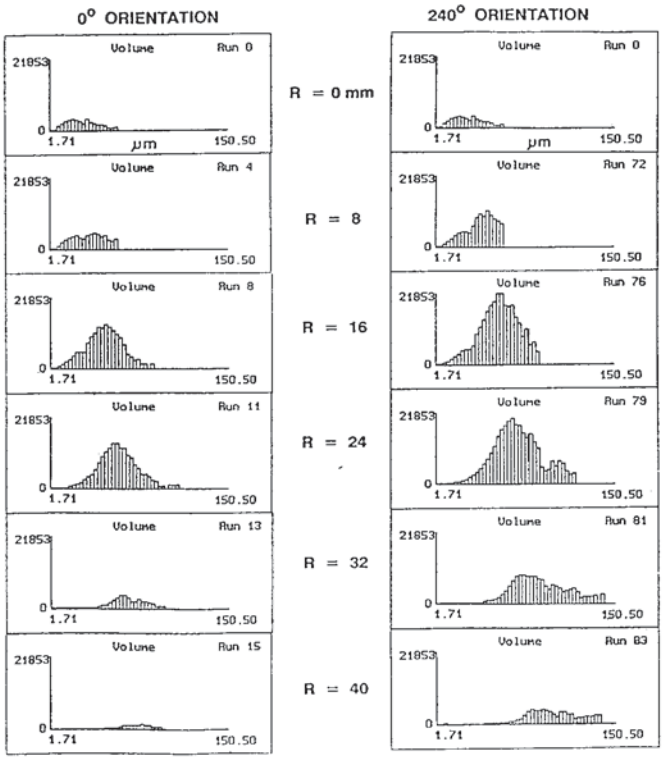

Fig. 15. Normalized Droplet Volume Distributions (100mm).

Figure 14 presents the normalized droplet distributions from select radial positions along the 0- and 240-degree orientations. The results show that the greatest population of droplets occurs at the centerline, and that these droplets tend to be small. In the region of greatest disparity in volume flux (radial positions greater than 16mm), relatively few drops exist. It is noteworthy that the 0-degree orientation possesses more droplets overall that does the 240-degree orientation.

Since the absolute number of droplets may not significantly affect volume flux, the count distributions in Figure 14 are presented in Figure 15 as volume distributions. Figure 15 shows that despite the fairly high numbers of small droplets at the centerline, relatively little volume is contributed by these drops. Examination of the volume distributions in the region of greatest volume flux disparity (radial positions greater than 16mm) indicates that a considerably greater number of large drops are present along the 240-degree orientation. Farther from the centerline, it is observed that the droplets present in this region are large, and that they are considerably larger and more numerous on the 240-degree orientation. This disparity in droplet distribution accounts for the flux differences not explained by the difference in size.

Drop Velocity. Figure 16 presents radial profiles of the gas and droplet mean axial velocities as a function of droplet size. Data are presented at locations where more than 100 drops within the size groupings selected were sampled (10,000 total droplets were sampled at each point). Hence, regions on Figure 16 where no data is presented for droplets indicates statistically insufficient number of drops of a given size range at that point.

Figure 16 shows that for droplets which are less than 75 μm in diameter, the profiles for either orientation are similar. The trends for drop size versus axial velocity are consistent, with smaller drops attaining the gas velocity sooner near the centerline. In regions away from the centerline (radial positions greater than 25mm), the droplets present possess enough momentum to exceed the gas velocity. In these regions, primarily larger drops exist which (1) have adequate momentum to overcome entrained air and travel away from the centerline, and (2) have the largest influence on the volume flux. The profile for the drops greater than 75 μm on the 240 degree traverse indicate that these drops are responsible for the greater radial spread in volume flux associated with this orientation. Hence, in the present case, the production of larger drops (diameters greater than 75 μm) existing along the 240 degree traverse is responsible for the increased radial spread in volume flux along that orientation.

Little dependency on size exists for the azimuthal component velocity (not presented for brevity), thus it appears that the slightly higher gas azimuthal velocity associated with the 240 degree orientation may also contribute to the increased radial spread. However, decoupling the two effects is not possible without further investigation.

a) 0-Degree Orientation

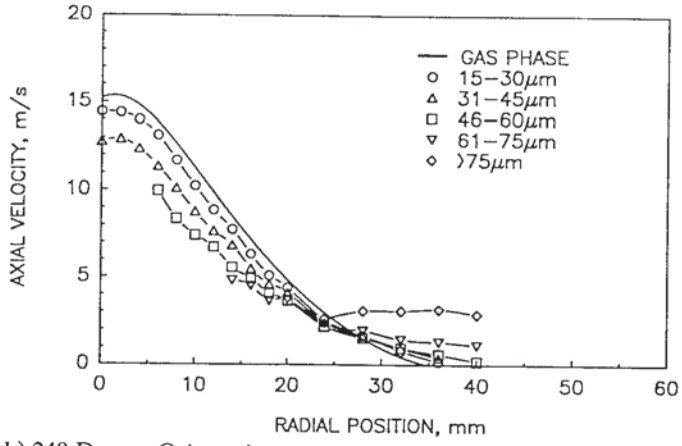

b) 240-Degree Orientation

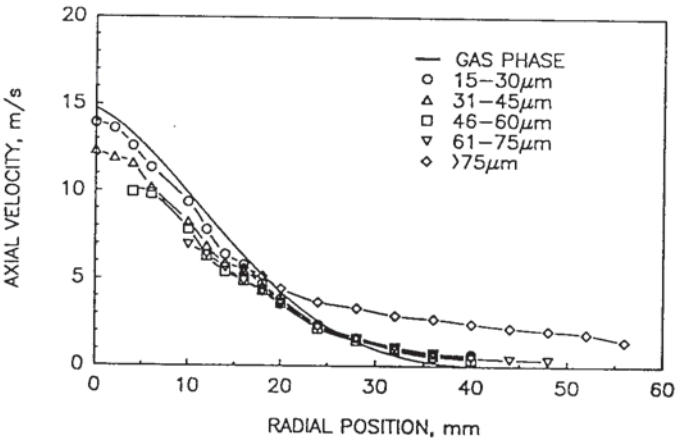

Fig. 16. Gas and Droplet Velocity Profiles (100mm).

SUMMARY

A precise study of the symmetry of the single and two phase flow produced by a practical air blast atomizer is conducted using phase Doppler interferometry. By conducting measurements of two velocity components and drop size distributions for each phase in a three dimensional manner, the degree of symmetry may be assessed, and the sources of asymmetries may be evaluated.

Conclusions drawn from this study are as follows:

- Two component phase Doppler interferometry is capable of distinguishing and measuring statistics for each phase in practical spray fields.
- In the present case, the single phase flow produced possesses a significant asymmetry which is considerably damped by the addition of liquid drops in a mass loading of 1.0.
- The addition of the second phase reduces the turbulence and spread of the continuous phase.
- The asymmetry in the volume flux in the present flowfield is mostly due to a disparity in the fuel injection distribution, which is manifested primarily in greater numbers of large drops which have adequate momentum to travel far from the centerline. Note that the size of the drops alone cannot account for the volume flux disparity.
- Variation in the gas azimuthal velocity field may influence the radial spread of the droplets and causes disparity in radial distribution of the fuel.
- The nature of the asymmetry in azimuthal gas velocity is different in the single and two phase flows, indicating that, although correlation exists between greater drop radial spread and high azimuthal gas velocities, direct correspondence between the two cases does not exist.
- It is necessary to measure statistics for both phases in two-phase flows to provide the information necessary to understand the transport processes occurring in flows of this type.

Overall, the study demonstrates the complexity of the two phase interaction and, in addition, shows that the tools necessary to understand the interaction are becoming available. In the present case, the dispersed phase dominates the continuous phase, and is clearly responsible for high local flux at 240 degrees. The disparity in radial spread is attributed to both dispersed and continuous phase asymmetry. In cases where air to fuel ratios of greater than one are considered, the influence of the continuous phase would become more important. The typical practice of line of sight average drop size, or even of making spatially resolved measurements of drop size does not provide necessary details regarding phase interaction. Also, steps should be taken to assess symmetry (via patternation for quick results) before data from a single profile is used to represent the overall behavior of the spray. Without such steps, conducting measurements along a single radial profile at several axial stations within practical flowfields presumes far too ideal a flow.

ACKNOWLEDGEMENTS

This work was supported, in part, by NASA Contract NAS3-24350 (J.D. Holdeman, Contract Monitor) in cooperation with the Allison Gas Turbine Division of General Motors. The participation of Brian Bird in the collection and analysis of the data is gratefully acknowledged. Howard Crum is to be applauded for assistance in the development and maintenance of the facility. Also, the help of Dr. W.D Bachalo in the specialized development and application of the instrument and software modifications is appreciated.

REFERENCES

Bachalo, W.D. and Houser, M.J., 1984, "Phase Doppler Spray Analyzer for the Simultaneous Measurement of Droplet Size and Velocity Distributions," *Optical Engineering*, Vol. 23, pp. 583-.

Bachalo, W.D., Rudoff, R.C., and Brena de la Rosa, A., 1988, "Mass Flux Measurements of a High Number Density Spray System Using the Phase Doppler Particle Analyzer," AIAA Paper No. 88-0236, 25th Aerospace Sciences Meeting, Reno, Nevada.

Bulzan, D., 1988, "Particle-Laden Weakly Swirling Free Jets: Measurements and Predictions," NASA TM 100881.

Dodge, L.G., Rhodes, D.J., and Reitz, R.D., 1987, "Drop-Size Measurement Techniques for Sprays: Comparison of Malvern Laser-Diffraction and Aerometrics Phase Doppler," *Applied Optics*, Vol. 26, pp. 2144-.

Jackson, T.A. and Samuelsen, G.S., 1987, "Droplet Sizing Interferometry: A Comparison of the Visibility and Phase Doppler Techniques," *Applied Optics*, Vol 26., pp. 2137-.

McDonell, V.G., Cameron, C.D., and Samuelsen, G.S., 1987 "Symmetry Assessment of an Air-Blast Atomizer," AIAA Paper No. 87-2136, 23rd Joint Propulsion Conference, San Diego, California, to appear, *AIAA Journal of Propulsion*.

McDonell, V.G. and Samuelsen, G.S., 1988, "Evolution of the Two-Phase Flow in the Near Field of an Air-Blast Atomizer Under Reacting and Non-Reacting Conditions," *Proceedings, Fourth International Symposium on Applications of Laser Anemometry to Fluid Mechanics*, Lisbon, Portugal.

McDonell, V.G., Wood, C.P., and Samuelsen, G.S., 1987, "A Comparison of Spatially Resolved Drop Size and Drop Velocity Measurements in an Isothermal Chamber and a Swirl Stabilized Combustor," *Twenty-First Symposium (International) on Combustion*, pp. 685-694.

McVey, J.B., Russell, S., and Kennedy, J.B., 1987, "High Resolution Patternator for the Characterization of Fuel Sprays," AIAA Journal of Propulsion, Vol 3, pp. 202-.

Mongia, H.C. and Reider, S.B., 1985, "Allison Combustion Research and Development Activities," AIAA Paper 85-1402, 21st Joint Propulsion Conference.

Mostafa, A.A., Mongia, H.C., McDonell, V.G., and Samuelsen, G.S., "On the Evolution of Particle-Laden Jet Flows: A Theoretical and Experimental Study," to appear, *AIAA Journal*.

Rudoff, R.C. and Bachalo, W.D., 1988, "Measurements of Droplet Drag Coefficients in a Polydispersed Turbulent Flow Field," AIAA Paper No. 88-0235, 25th Aerospace Sciences Meeting, Reno, Nevada.

Young, B.W. and Bachalo, W.D., 1987, "The Direct Comparison of Three 'In-Flight' Droplet Sizing Techniques for Pesticide Spray Research," *Proceedings, International Symposium on Optical Particle Sizing: Theory and Practice*, Rouen, France.